Dynamic Control of Full-Colored Emission and Quenching of Photoresponsive Conjugated Polymers by Photostimuli

*Kazuyoshi Watanabe, Hiroyuki Hayasaka, Tatsuaki Miyashita, Kenta Ueda, and Kazuo Akagi**

A series of photoresponsive and full-colored fluorescent conjugated copolymers is synthesized by combining phenylene- and thienylene-based main chains with photochromic dithienylethene (DE) side chains. Solutions and cast films of the polymers exhibit various colored fluorescence in visible wavelengths of 400–700 nm corresponding to emissions of the conjugated main chain. The fluorescence is reversibly photoswitched between emission and quenching through DE photoisomerization using external stimuli from ultraviolet and visible light irradiation. The reprecipitation method with ultrasonication enables the polymers to form spherical aggregates with diameters of 20–70 nm in water. After investigating and comparing the optical properties, the resulting nanosphere solutions are assumed to exist in an intermediate state between an isolated state (i.e., in solution) and an aggregated state in cast film. The majority of the nanosphere solutions also exhibit the same photoswitchable fluorescence behavior as those in the solutions and the cast films. The results demonstrate that the visible fluorescence of the conjugated copolymers is reversibly switchable between emission and quenching using the photoisomerizing DE side chain regardless of the fluorescent colors and the polymer chain aggregation.

1. Introduction

Aromatic π-conjugated polymers (ACPs) are promising candidates for advanced functional materials and are expected to be applied in such organic devices as organic light-emitting diodes, organic field-effect transistors, organic photovoltaic cells, and chemical biosensors due to their semiconductive and optoelectronic properties.[1–8] The ACPs exhibit various colored fluorescence in the visible region due to changes in the main chain structures because their properties are fundamentally determined by the primary structure of the conjugated backbones. Furthermore, the fluorescent property can be modified and functionalized by controlling the secondary or higher-ordered structures of the main chains in an aggregated state. It is well known that linearly aligned and helically π-stacked ACPs show linear and circular dichroism in luminescence, respectively.[9–13] In another case, aggregation-induced emission (AIE) and aggregation-enhanced emission (AEE) characteristics were reported in selected ACPs.[14–16] Therefore, it is of great interest to investigate ACPs in the aggregated state that are quite different from those the isolated chain state.

The polymer nanosphere solution can be treated as an intermediate state between a solution state and a solid film state because the polymer nanoparticles uniformly disperse in a solvent, similar to their behavior in solution, whereas the polymer chains aggregate with each other, similarly to their behavior in a solid film. In other words, the polymer nanosphere solution can be regarded as a dispersed nano-ordered crystalline polymer system. This bilateral character of the nanosphere solution causes the polymer to exhibit high processability and fluidity as well as aggregation effects. In addition, the polymer nanosphere solution enables quantitative analysis of the aggregated state of polymers from the spectroscopic point of view. Hence, the polymer nanosphere solution is useful for understanding the aggregation effect on ACPs as compared with the solution and solid film states.

Dynamic control of the fluorescence of ACPs using an external light stimulus is of particular interest because such photoresponsive polymers are essential for next-generation optoelectronic materials. Dithienylethene (DE) derivatives[17–20] are one class of the most attractive photoresponsive materials because of their outstanding fatigue resistance, thermal stability, and ability to undergo conformational changes between open and closed forms via photoisomerization, and therefore they are regarded as promising materials for the fabrication of photodynamically controllable luminescent devices[21,22] as well as photodynamically color-tunable systems.[23–27] The DE derivatives are also known to display luminescent color changes via photoisomerization.[20,28–37] Similarly, conjugated polymers that contain DE moieties in the polymer backbones exhibit photochromism.[20,38–41] The chromism in both absorption and luminescence of the conjugated polymers is attributed to structural changes in the conjugated backbones resulting from the DE photoisomerization. Hence, it is necessary to properly design the molecular structure to realize the desired switching behavior and fluorescent colors.

It is well known that in ACP nanoparticles doped with luminescent dopants, the ACP fluorescence is almost completely quenched and the fluorescence of the dopant is mainly

K. Watanabe, Dr. H. Hayasaka, T. Miyashita,
K. Ueda, Prof. K. Akagi
Department of Polymer Chemistry
Kyoto University, Katsura
Nishikyo-ku, Kyoto 615–8510, Japan
E-mail: akagi@fps.polym.kyoto-u.ac.jp

DOI: 10.1002/adfm.201500136

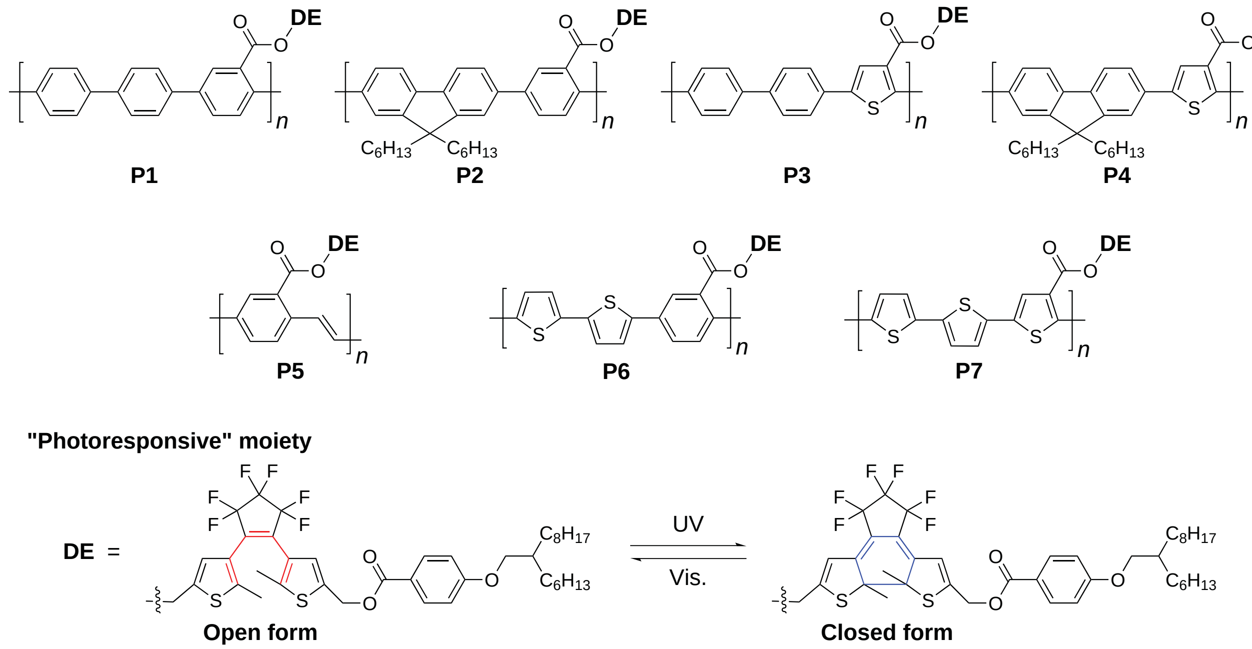

Scheme 1. Structures of photoresponsive conjugated polymers.

observed.[42] This is due to the intraparticle energy transfer from the ACP backbone to the dopant. Thus, it was previously reported that the ACP nanoparticles doped with photochromic dyes showed reversible fluorescence photoswitching between emission and quenching by photoisomerization of the dyes upon irradiation of external light stimuli.[42–45] On the other hand, it was also reported that the ACPs incorporated with photochromic moieties showed reversible photomodulation of the fluorescence by using light stimuli.[46–48] In these polymer systems, the fluorescent moiety is independent of the photochromic moiety, resulting in high flexibility on the molecular design.

By introducing the DE moiety into the side chains of ACPs, the polymer fluorescence in solution and solid film was switchable between emission and quenching via reversible DE photoisomerization. In previous work, we reported the photodynamic ON/OFF switching of linearly polarized luminescence (LPL) in macroscopically aligned ACPs and also that of circularly polarized luminescence (CPL) in helically π-stacked ACPs using UV–vis light stimuli.[49,50] In these cases, the fluorescent conjugated backbones of the polymers were unchanged before and after DE photoisomerization, and therefore, the interchain structures were maintained. In addition, this material offers the advantage of free design of the fluorescent color because the fluorescent polymer backbone and the photoisomerized DE side chain are independent of each other from the viewpoint of the π-electronic structure. Very recently, we reported that three types of ACPs with the DE side chains showed red-, green-, and blue-colored fluorescence in the nanosphere solution, and they exhibited photoswitching behavior between emission and quenching by external light stimuli.[51] However, the red-colored fluorescent ACP showed bluish purple-colored fluorescence in chloroform solution although it exhibited red-colored fluorescence in nanosphere solution and solid film. This is because the main chain of the red-colored fluorescent ACP consists of a polyfluorene backbone containing a very small amount of 4,7-di(2-thienyl)-2,1,3-benzothiadiazole (DBT) moiety, and the red-colored fluorescence of the DBT moiety is only observable in the aggregated state. This means that the photodynamic ON/OFF switching behavior of full-colored fluorescence has not been completely achieved in the isolated chain state such as in the chloroform solution.

In this work, we designed and synthesized several types of photoresponsive ACPs by incorporating a DE side chain into various conjugated main chains, i.e., poly(*p*-terphenylene) [**P1**], poly(fluorene-phenylene) [**P2**], poly(biphenylene-thienylene) [**P3**], poly(fluorene-thienylene) [**P4**], poly(*p*-phenylene-vinylene) [**P5**],[49] poly(bithienylene-phenylene) [**P6**],[49] and poly(terthiophene) [**P7**] (**Scheme 1**). The polymers exhibited various blue–red colored fluorescence corresponding to the conjugated length of the main chains. In solution and solid film, it was successfully demonstrated that the fluorescence of ACPs in the whole visible region was reversibly switchable between emission and quenching through photoisomerization of the DE side chains regardless of the fluorescence wavelengths (**Figure 1**). The quenching efficiency in cast films was higher than that in solutions as a result of the aggregation effect. The reprecipitation method with ultrasonication enabled the polymers to form spherical aggregates with diameters of 20–70 nm in water. The resulting nanosphere solutions exhibited moderate fluorescent properties between those of solutions and solid films, and the fluorescence was also photoswitchable, except for the red-colored fluorescence of **P7**. Herein, we conducted a comprehensive investigation of the photoswitchable full-colored fluorescence of ACPs bearing DE side chains in both the isolated chain and the aggregated states.

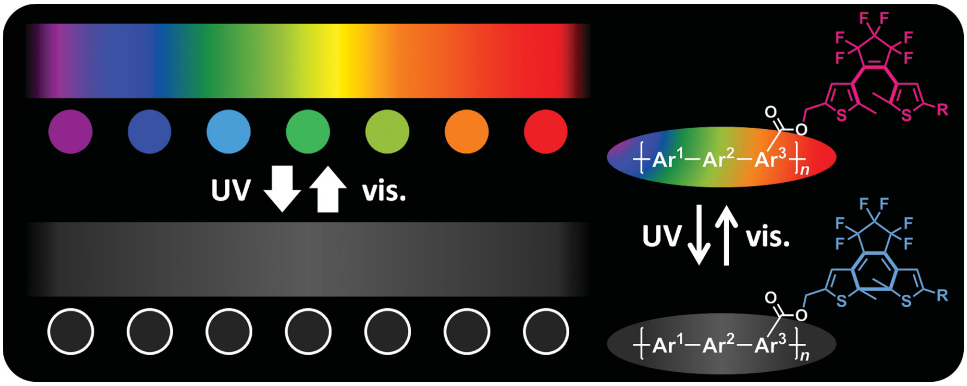

Figure 1. Scheme of photoswitching behavior of multicolored fluorescence between emission and quenching by using DE photoisomerization.

2. Results and Discussion

2.1. Synthesis and Characteristics of Photoresponsive Conjugated Polymers

The synthetic routes of the photoresponsive monomers and polymers are shown in **Scheme 2**. 2,5-Dibromobenzoic acid and 2,5-dibromo-3-thenoic acid were esterified with the DE derivative **2** via Mitsunobu reaction to give **3** and **4**, respectively. Esterification of the intermediate products with **1** in the presence of both *N,N'*-dicyclohexylcarbodiimide (DCC) and 4-(dimethylamino)pyridine (DMAP) yielded the photoresponsive monomers, **M1** and **M2**, respectively. The photoresponsive conjugated polymers **P1–P4** were synthesized via a Suzuki coupling reaction between the monomers and diborate monomers, i.e., 4,4′-biphenyldiboronic acid cyclic ester and 9,9-dihexylfluorene-2,7-diboronic acid cyclic ester, in the presence of tetrakis(triphenylphosphine)palladium(0) [Pd(PPh$_3$)$_4$] as a catalyst. The **P5–P7** polymers were synthesized through a Stille coupling reaction between the monomers and distannyl monomers, i.e., 1,2-bis(tributylstannyl)ethylene and 5,5′-bis(trimethylstannyl)-2,2′-bithiophene, in the presence of tris(dibenzylideneacetone)dipalladium(0) [Pd$_2$(dba)$_3$] and tri-2-furylphosphine [(2-furyl)$_3$P] as catalysts.

The molecular structures of the monomers and the polymers were confirmed using nuclear magnetic resonance (NMR) measurements, mass spectrometry, and elemental analysis. All synthesized polymers were fusible and soluble in such organic solvents as tetrahydrofuran (THF), toluene, and chloroform (CHCl$_3$). **Table 1** shows the average molecular weights of the polymers as evaluated by gel permeation chromatography (GPC). The number- and weight-average molecular weights (M_n and M_w) of the polymers range from 1.1×10^4 to 2.0×10^4 and 1.2×10^4 to 1.5×10^5, respectively, resulting in a polydispersity index (PDI, M_w/M_n) of 1.1–7.5. The degree of polymerization (DP) was estimated as 10–19 using the M_n values. The DE moiety in the side chains successfully photoisomerized from the open form to closed form upon irradiation by UV light ($\lambda = 254$ nm). The level of DE conversion to closed form in a photostationary state (PSS) was estimated as 42%–47% by using ^{1}H NMR results (see the Experimental Section for more detail). In this work, a PSS is an equilibrium state between the open form and the closed form of the DE moiety under UV irradiation. After subsequent irradiation with visible light ($\lambda > 400$ nm), all proton signals corresponding to the DE open form were regenerated. These results indicated that reversible photoisomerization of DE moiety occurred even in the polymer side chains.

2.2. Absorption and Fluorescence of P1–P7 Solutions and Cast Films

First, we investigated the optical properties of the **P1–P7** solutions and cast films. The absorption peaks of **P1–P7** in CHCl$_3$ solution ($c = 4.0 \times 10^{-5}$ M) and cast film are summarized in **Table 2**. The polymer cast films were prepared from CHCl$_3$–toluene solutions of the corresponding polymers. As shown in **Figure 2**a, the polymer solutions in an open state showed various absorption bands in the visible region of 300–600 nm, which corresponds to π–π* transition of the polymer conjugated backbone. The polymer cast films showed absorption bands in a longer wavelength region than those of the CHCl$_3$ solutions (Figure 2b) because the effective conjugated length of the polymer main chains were increased in the solid state. More specifically, the absorption bands of **P1–P7** were red-shifted by 11, 0, 19, 14, 11, 35, and 40 nm, respectively (see Table 2). It is worth noting that the thienylene-containing polymers of **P3**, **P4**, **P6**, and **P7** exhibited larger red shifts in absorption than those of the thienylene-free polymers **P1**, **P2**, and **P5**. This effect results from the high π-stacking feature of the thienylene ring, which enhances the coplanarity of the polymer conjugated backbone in a solid state. This observation is also supported by the fact that the degree of red shift increases with the number of thienylene rings in a polymer repeating unit, i.e., the absorption peak shift is 0–11 nm for thienylene-free polymers **P1**, **P2**, and **P5**; 14–19 nm for monothienylene-containing polymers **P3** and **P4**; 35 nm for the bithienylene-containing polymer **P6**; and 40 nm for terthienylene-containing polymer **P7**.

Figure 2c,d displays the photoluminescence (PL) spectra of the polymers in the open state with excitation wavelengths at either 350 or 380 nm. The CHCl$_3$ solutions and cast films of the polymers exhibited various colored fluorescence that corresponded to π*–π transition of the polymer conjugated backbone. As shown in **Figure** 2c,d, **3**, the fluorescent color of the polymer solutions and cast films changed from blue to red with an increasing number of thienylene rings in the repeating unit,

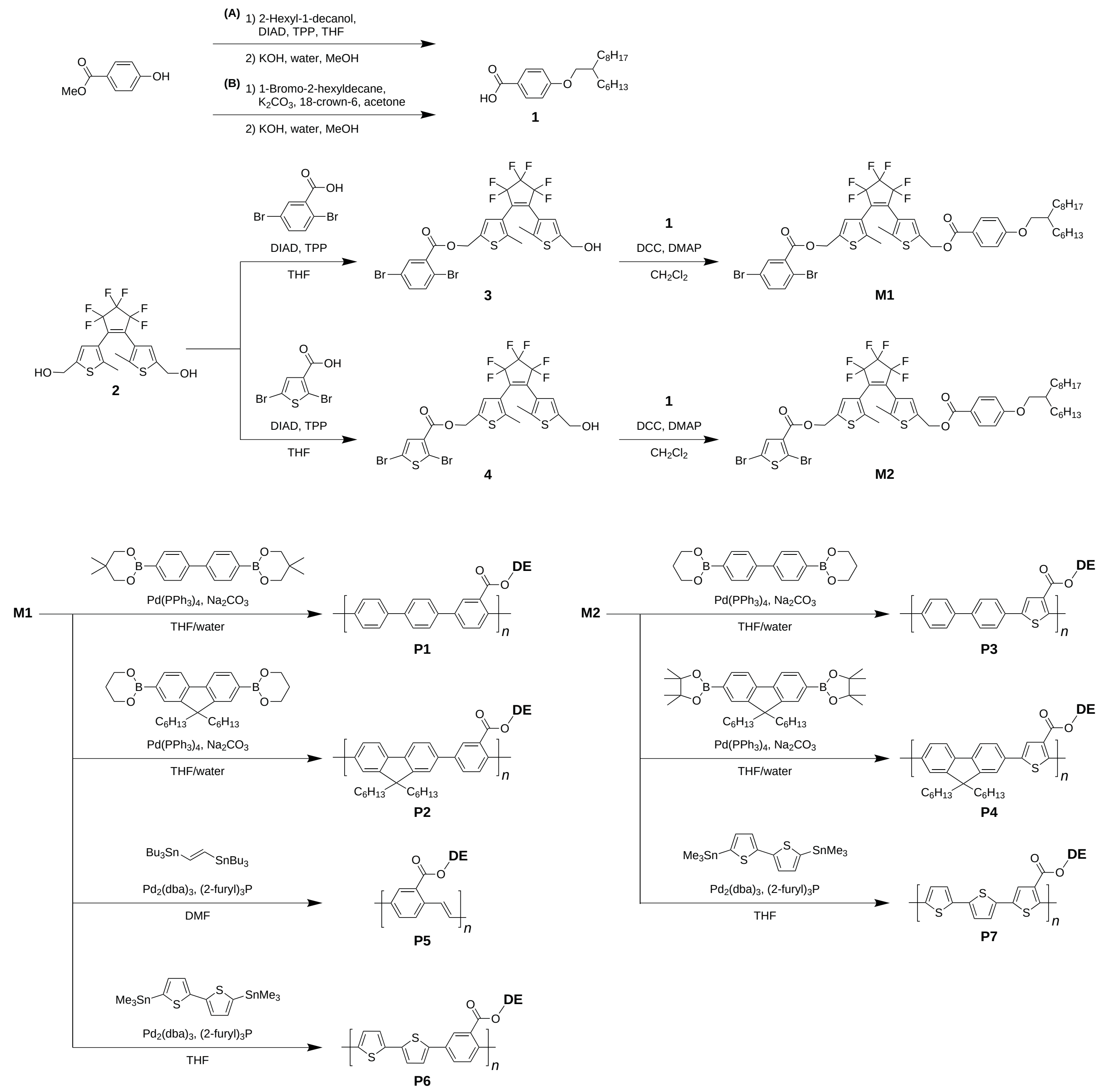

Scheme 2. Synthetic routes of photoresponsive conjugated polymers, **P1**–**P7**.

except for the PPV derivative **P5**. Specifically, thienylene-free **P1** and **P2** showed blue fluorescence, monothienylene-containing **P3** and **P4** displayed bluish-green fluorescence, bithienylene-containing **P6** displayed green and yellow fluorescence, and terthienylene-containing **P7** displayed red fluorescence. The fluorescence peak wavelengths of the polymers are listed in **Table 3**. This result also indicates that the thienylene ring enhances the coplanarity of the polymer main chain, and hence, the effective conjugated length. The fluorescence quantum yields of the polymer solutions in the open state (Φ_{open}) were evaluated using quinine sulfate in 1.0 M sulfuric acid as a standard, as summarized in Table 3. Thienylene-free **P1** and **P2**, which consist of phenylene and fluorene rings, showed high Φ_{open} values of 62% and 85%, respectively. However, thienylene copolymers **P3**, **P4**, and **P6** and PPV derivative **P5** showed lower Φ_{open} values of 23%–26%. Furthermore, PT derivative **P7** showed a significant low Φ_{open} value of 5%, which might be due to a so-called "concentration quenching in fluorescence" phenomenon resulting from the high π-stacking feature of the thienylene rings.[52–54]

2.3. Photoswitching Behavior in Absorption and Fluorescence of P1–P7 Solutions and Cast Films

Next, we investigated the absorption and fluorescence changes upon irradiation by external light sources for **P1**–**P7** solutions

Table 1. Molecular weights of **P1**–**P7** and level of DE conversion to closed form in a PSS.

Polymer	M_n	M_w	M_w/M_n	DP[a)]	Level of DE conversion to closed form in a PSS[b)] [%]
P1	10 700	12 200	1.1	10	45
P2	15 500	31 000	2.2	12	45
P3	20 000	148 000	7.5	19	42
P4	20 000	150 000	7.4	16	42
P5[c)]	13 000	36 000	2.7	14	47
P6[c)]	14 200	18 800	1.3	14	42
P7	17 000	51 000	3.0	16	45

[a)] Degree of polymerization; [b)] The values were estimated by using ^{1}H NMR results of the polymers in $CDCl_3$; [c)] Previous study.[49]

and cast films. **Figure 4** shows the spectral changes of the $CHCl_3$ solution of **P2** in an open state and a PSS. As shown in Figure 4a, the absorption band at approximately 255 nm gradually decreased in intensity as the DE moiety changed from the open form to the closed form upon irradiation by UV light (λ = 254 nm). At the same time, other absorption bands at approximately 360 and 520 nm increased in intensity, which correspond to the DE closed form. The absorption changes stopped after 50 s of UV irradiation because **P2** reached the PSS. Subsequent irradiation by visible light (λ > 400 nm) for 5 min caused photoisomerization of the DE moiety from the closed form to the open form, resulting in regeneration of the absorption spectrum of **P2** in the open state. The inserted images show the color change of the **P2** solution in the open state and PSS. All of the other polymer solutions also exhibited the same photoswitching behavior in absorption, as shown in Figure S1 (Supporting Information). It is worthy to emphasize that the DE moiety in the polymers can photoisomerize by external light stimuli although all the absorption bands overlap those of the polymer conjugated main chains (see Figure S7a,b, Supporting Information). This suggests that the DE moiety receives photonic energy enough to be photoisomerized even if the conjugated backbone coexists.

Figure 4b shows the fluorescent change of the $CHCl_3$ solution of **P2** via DE photoisomerization. The blue fluorescence band of **P2** in the open state drastically decreased in intensity upon irradiation by UV light (λ = 254 nm) and was completely quenched when **P2** reached the PSS. The various colored fluorescence of the other polymer solutions was also quenched by UV irradiation (see Figure 3 and Figure S2, Supporting Information). The fluorescence intensity ratios between the open state and PSS (I_{open}/I_{PSS}) of the polymer solutions were estimated as 50–190 and are summarized in Table 3. Fluorescence quenching might occur due to efficient energy transfer from the excited polymer conjugated backbone to the DE side chain in the closed form, and the DE side chain subsequently releases the energy through nonradiative transition from the excited to ground states.[49–51] The quenched fluorescence was regenerated by irradiation with visible light (λ > 400 nm), which photoisomerized the DE closed form to the open form. As a result, $CHCl_3$ solutions of the polymers exhibited reversible photoswitching behavior in fluorescence between emission and quenching using external UV and visible light stimuli.

Similar to the $CHCl_3$ solutions, **P1**–**P7** cast films also exhibited reversible spectral changes in absorption and fluorescence (Figures S3 and S4, Supporting Information). Interestingly, the polymer cast films showed the distinct photoswitching behavior in fluorescence with high I_{open}/I_{PSS} values of 80–790 (see Table 3). The I_{open}/I_{PSS} values of the cast films are larger than those of the $CHCl_3$ solutions, indicating that the energy of the excited polymer backbone efficiently transfers to the DE side chain in a solid state, i.e., in a cast film where the polymer chains are located close to each other. Figure 3 shows photographs of the $CHCl_3$ solutions and cast films of **P1**–**P7** in the open state and the PSS, which visually demonstrates the reversible photoswitching behavior of various colored fluorescence.

Table 2. Absorption peaks of $CHCl_3$ solutions, nanosphere solutions, and cast films of **P1**–**P7** in an open state.

Polymer	$CHCl_3$ solution[a)]	Nanospheres solution		Cast film	
	λ_{max} [nm]	λ_{max} [nm]	$\Delta\lambda_{max}$[b)] [nm]	λ_{max} [nm]	$\Delta\lambda_{max}$[b)] [nm]
P1	342	353	11	353	11
P2	358	359	1	358	0
P3	370	385	15	389	19
P4	394	402	8	408	14
P5	414	417	3	425	11
P6	426	450	24	461	35
P7	508	531	23	548	40

[a)] Polymer concentration: 4.0×10^{-5} M; [b)] Absorption peak shift from the λ_{max} of the polymer $CHCl_3$ solution.

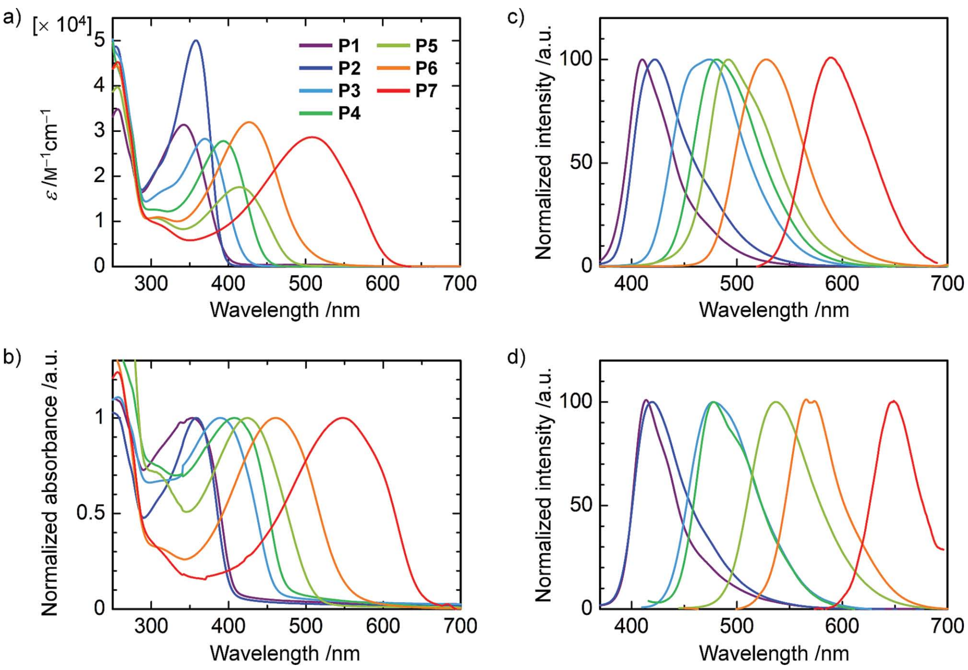

Figure 2. a,b) UV–vis absorption and c,d) normalized PL spectra of **P1**–**P7** in an open state. a,c) $CHCl_3$ solutions ($c = 4.0 \times 10^{-5}$ M) and b,d) cast films. Excitation wavelength: 350 nm for all $CHCl_3$ solutions and **P1** and **P2** cast films; 380 nm for **P3**–**P7** cast films.

It should be noted that the DE moiety in an open state has no absorption band in the region of 350–800 nm (see Figure S8, Supporting Information), and hence no photoisomerization occurs on the DE moiety upon the irradiation of excitation light of $\lambda = 350$ and 380 nm. On the other hand, the DE moiety in a PSS has an absorption band covering the wavelength of

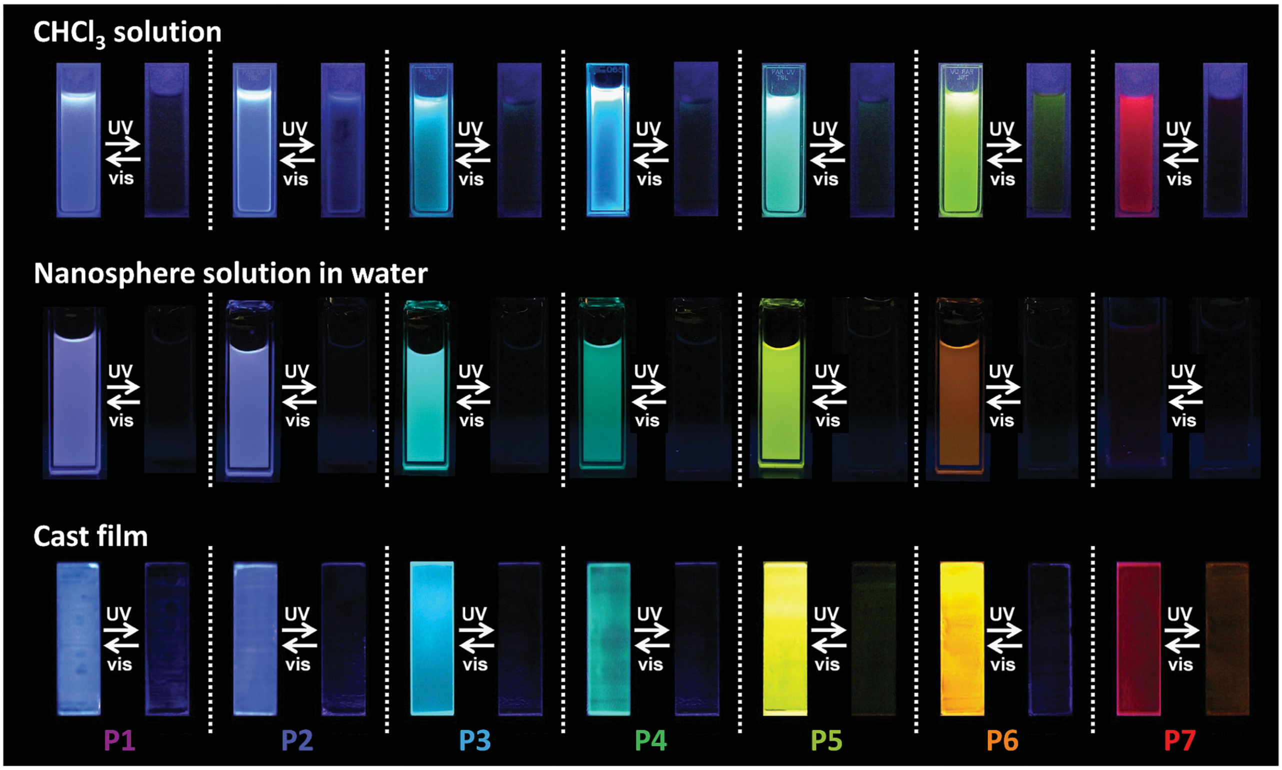

Figure 3. Photoswitching behavior between emission and quenching of full-colored fluorescence of **P1**–**P7** $CHCl_3$ solutions (upper), nanosphere solutions (middle), and cast films (lower) by UV and visible light stimuli. Excitation wavelength: $\lambda = 370$ nm.

Table 3. Fluorescence properties of **P1**–**P7** in $CHCl_3$ solution, nanosphere solution, and cast film.

Polymer	$CHCl_3$ solution[a]			Nanosphere solution		Cast film	
	Em_{max}[b] [nm]	Φ_{open}[c] [%]	I_{open}/I_{PSS}[d]	Em_{max}[b] [nm]	I_{open}/I_{PSS}[d]	Em_{max}[b] [nm]	I_{open}/I_{PSS}[d]
P1	410[e]	62	120	414[e]	140	412[e]	490
P2	422[e]	85	190	420[e]	320	419[e]	790
P3	474[e]	26	80	481[f]	270	478[f]	360
P4	480[e]	24	50	480[f]	235	478[f]	290
P5	492[e]	24	120	539[f]	375	536[f]	530
P6	528[e]	23	90	571[f]	180	575[f]	320
P7	593[e]	5	60	648[f]	30	647[f]	80

[a] Polymer concentration: 4.0 × 10^{-5} M; [b] Fluorescence peak of the polymer in an open state; [c] Fluorescence quantum yield in an open state evaluated by using quinine sulfate in 1.0 M sulfuric acid as a standard; [d] Fluorescence intensity ratio between the open state and PSS; [e] Excitation wavelength: 350 nm; [f] Excitation wavelength: 380 nm.

300–400 nm. Thus, the DE moiety may partially photoisomerize from the closed to open form under irradiation of the excitation light, resulting in changes in the absorption spectra. To avoid the photoisomerization, the photoluminescence spectra of the polymers in a PSS were measured in a short time (less than 14 s).

2.4. Fatigue Resistance in Fluorescence Photoswitching of Polymers

We investigated the fatigue resistance of all the polymer films. As shown in Figure S9 (Supporting Information), the photoswitching behavior was maintained after repeating the photoisomerization cycle 5 times although the PL intensity decreased to 2.6%–25.4%. Moreover, Figure S10 (Supporting Information) shows spectral changes in UV–vis absorption of the polymer films in an open state. As indicated by the black arrows, the absorption band at 250 nm, corresponding to the DE moiety, also decreased in intensity with repeating the photoisomerization cycle. On the other hand, the absorption bands corresponding to the conjugated main chains were unchanged, except the case of **P5**. These results indicate that the DE moiety partially changed into an unphotochromic byproduct, suppressing the full regeneration of the polymer fluorescence. Because the UV light (λ = 254 nm) used for DE photoisomerization has relatively high energy and can damage the photochromic conjugated structure of DE, the unphotochromic byproduct might be formed. This is also supported by the spectral change in UV–vis absorption of the DE moiety, **2**, during the photoisomerization cycle (Figure S7a,b, Supporting Information). In both the open state and PSS, the absorption band at 250 nm decreased in intensity with repeating the photoisomerization cycle, whereas the absorption band at 300 nm increased in intensity. This result indicates that the DE moiety gradually changed into an unphotochromic byproduct. The extinction coefficient at 518 nm, which corresponds to the DE closed form, also decreased to 30.2% after 5 cycles of the photoisomerization (see Figure S7c, Supporting Information), implying a loss of the photochromic property. The decrease in fatigue resistance of all the polymers, therefore, is due to the degradation of the DE moiety. Interestingly, the absorption band of **P5** main chain decreased in intensity and blue-shifted with every photoisomerization cycle, as shown Figure S10e, Supporting Information (green arrow). Such a change in absorption denotes a decrease in the conjugated length of **P5** main chain, indicating that the polymer conjugated backbone is photo-oxidized by irradiating UV light. However, **P5** showed relatively better

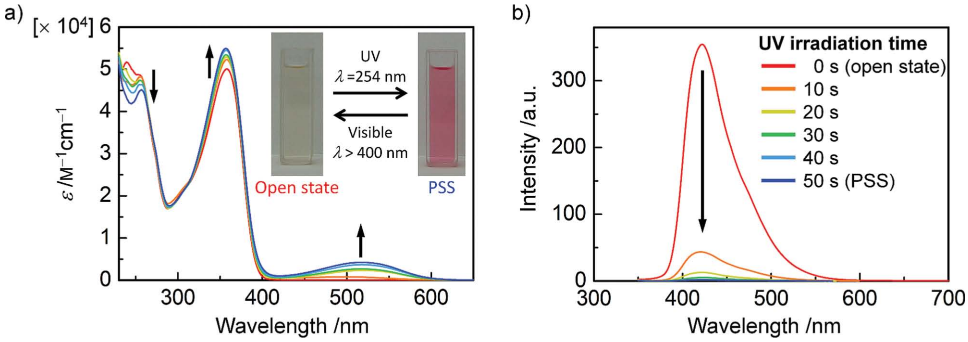

Figure 4. Spectral changes in a) UV–vis absorption and b) PL spectra of **P2** $CHCl_3$ solution (c = 4.0 × 10^{-5} M) under UV irradiation (λ = 254 nm). Insets show the photo images of **P2** $CHCl_3$ solution in the open state and PSS. Excitation wavelength: 350 nm.

Figure 5. a) Schematic procedure of reprecipitation method. b) Photo images of **P1**–**P7** nanosphere solutions in water.

fatigue resistance from the viewpoint of PL intensity, as shown in Figure S9 (Supporting Information). Thus, in this case, the photoswitching behavior of the fluorescence is affected by the degradation of DE moiety rather than the photo-oxidization of the conjugated main chain.

2.5. Preparation Method for Polymer Nanosphere Solutions

Polymer nanospheres dispersed in water were prepared using the reprecipitation method with ultrasonication.[55] A schematic of the procedure is shown in **Figure 5**a, and the process details are described as follows. Solutions of the polymers (0.31–0.48 mg, see **Table 4**) in THF (1.5 mL) were added dropwise into water (10 mL) at 0 °C under ultrasonication using an ultrasonic homogenizer (130 W, 20 kHz). The THF solvent was removed under reduced pressure at 55 °C to give the polymer nanosphere solutions in water. Figure 5b shows photo images of **P1**–**P7** nanosphere solutions. The polymer nanospheres remained dispersed in water even if they were held at room temperature for several months, indicating the high stability of the nanospheres.

2.6. Morphology of Polymer Nanospheres

The morphology of the polymer nanospheres was observed using scanning electron microscopy (SEM). **Figure 6** shows the SEM images of **P1**–**P7** nanospheres, which indicate that all polymers form spherical aggregates with an average particle size of 20–70 nm in diameter. The size distribution was also estimated using the SEM images, as summarized in Table 4.

2.7. Photoswitching Behavior in Absorption and Fluorescence of Polymer Nanospheres

Figure 7 shows the UV–vis absorption and PL spectra of nanosphere solutions of **P1**–**P7** in the open state. Similar to both of the $CHCl_3$ solutions and the cast films, the nanosphere solutions showed absorption and fluorescence bands corresponding to the π–π^* and π^*–π transitions of the polymer conjugated backbones. Thus, the peak wavelengths in both absorption and fluorescence were red-shifted with the increase in the effective conjugated length of the polymer backbone in the order of **P1**–**P7**. Namely, the fluorescence color gradually changed from blue to red. The absorption and fluorescence peak wavelengths are summarized in Tables 2 and 3.

Interestingly, the absorption peaks in the nanosphere solutions exhibited intermediate values between those of the solutions and the cast films. This result implies that the nanosphere solution represents an intermediate state between an isolated state and an aggregated state. At the same time, the fluorescence peak wavelengths were similar to those in the cast films. It is well known that the fluorescence of conjugated polymers involve quasi-localized chromophores in the polymer backbone.[56,57] In addition, the energy in the excited conjugated backbone transfers intramolecularly and is finally trapped in low-transition-energy regions, the so-called "exciton traps." Thus, the fluorescence spectra tend to reflect the fluorescent property of the exciton traps rather than that of the average of the entire conjugated backbone.[58] Hence, these

Table 4. Conditions for nanosphere preparation and the particle size of the nanospheres.

	Conditions for nanosphere preparation[a)		Particle size [nm]	
	Polymer amount		Average	Distribution
	[mg]	[μmol]		
P1	0.479	0.47	50	30–80
P2	0.464	0.38	40	30–60
P3	0.452	0.44	45	30–50
P4	0.312	0.25	60	40–75
P5	0.398	0.44	70	50–90
P6	0.428	0.41	20	15–50
P7	0.412	0.39	35	25–50

[a)] The polymers were dissolved in THF (1.5 mL) and then added dropwise into water (10 mL) under ultrasonication.

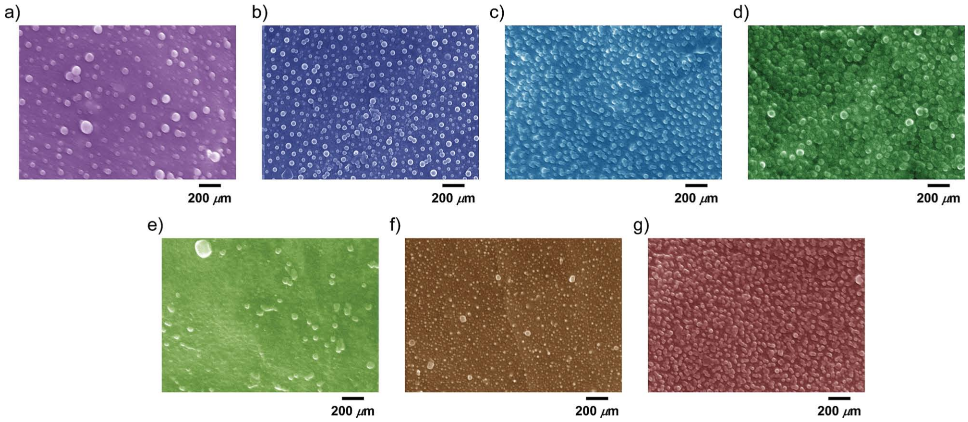

Figure 6. SEM images of polymer nanospheres. a) **P1**, b) **P2**, c) **P3**, d) **P4**, e) **P5**, f) **P6**, and g) **P7**.

results indicate that **P1–P7** nanospheres have exciton traps similar to those of the cast films because the polymers exist in an aggregated state in both the nanosphere solutions and the cast films.

The photoinduced spectral changes in both absorption and fluorescence were also investigated. **Figure 8**a shows the absorption change of the **P2** nanosphere solution induced by external light stimuli. The absorption spectra show that the band at approximately 255 nm decreased in intensity with irradiation by UV light, whereas the bands at approximately 350 nm and 520 nm increased. This result indicates that the DE side chains photoisomerize from the open form to the closed form even in the polymer nanospheres. Subsequent irradiation by visible light regenerated the original absorption spectrum of **P2** in the open state through reverse photoisomerization of the DE moiety. Figure 8b shows the fluorescence change of the polymer nanosphere solution. Similarly to the $CHCl_3$ solutions and the cast films, the fluorescence of **P2** nanospheres were quenched by UV irradiation and subsequently regenerated upon irradiation with visible light. The other nanosphere solutions of **P1** and **P3–P7** also exhibited the same behavior in both absorption and fluorescence regardless of the fluorescent colors (see Figure 3, Figures S5 and S6, Supporting Information). These results successfully demonstrated that the multi-colored fluorescence of the polymer nanospheres was photoswitchable between emission and quenching using external light stimuli. In addition, the I_{open}/I_{PSS} values were evaluated as 30–375, as summarized in Table 3, and represent intermediate values between those of the solutions and the cast films, except for **P7** (see **Figure 9**). This result also implies that the nanosphere solution is an intermediate state between an isolated state and an aggregated state.

It is worth noting that the red-colored fluorescence of **P7** nanosphere solution is unexpectedly weak in intensity, and therefore, it is difficult to visually observe the fluorescence photoswitching on a photo image (Figure 3). This is due to the high π-stacking feature of the PT backbone consisting only of thienylene rings with a planar structure, which causes a decrease in the fluorescence intensity in a solid state. In addition, the energy in the excited PT backbone is easily decayed due to the polarizable environment of the surrounding water solvent. The red-colored fluorescence of **P7** nanosphere solution is therefore too weak to be observed.

2.8. Mechanism of Fluorescence Quenching

As shown in Figure S8 (Supporting Information), the absorption band of the DE moiety **2** in a PSS overlaps the fluorescence bands of all the polymers although the absorption band of **2** in an open state does not. This is because the absorption band at 518 nm corresponding to the DE closed form extends over the visible region. It is therefore anticipated that the fluorescence of the polymers may be quenched through an energy transfer

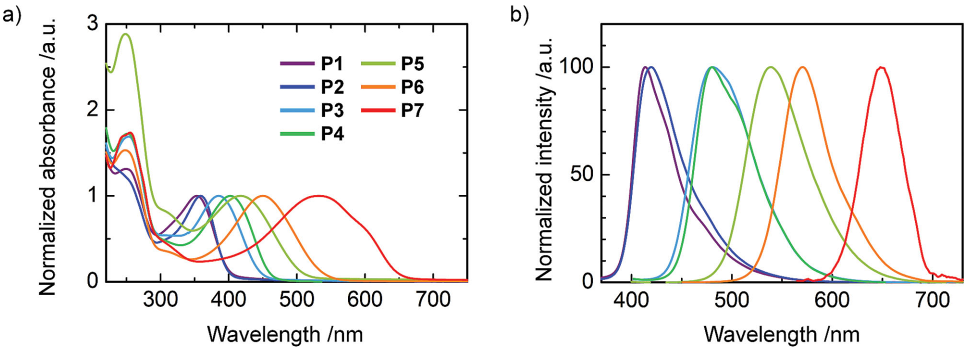

Figure 7. a) UV–vis absorption and b) normalized PL spectra of **P1–P7** nanosphere solutions in water.

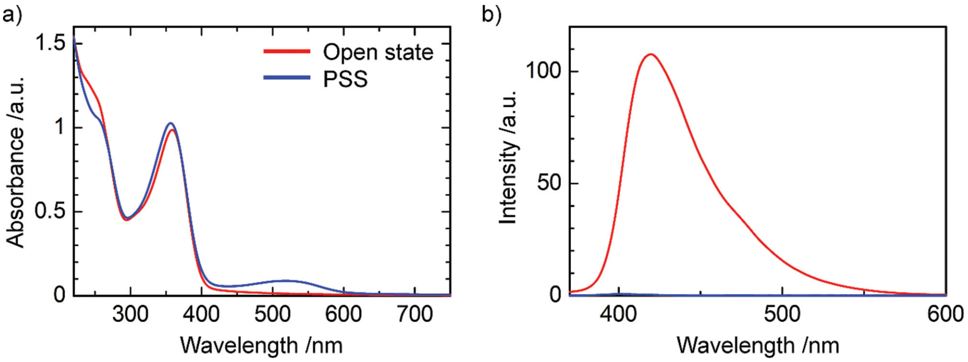

Figure 8. a) UV–vis absorption and b) PL spectra of polymer nanosphere solutions of **P2** in an open state and a PSS.

such as Förster resonance energy transfer (FRET) from the polymer conjugated backbone to the DE closed form, which requires the spectral overlap between the luminescence of donor (polymer conjugated backbone, herein) and the absorption of acceptor (DE closed form).

Furthermore, we investigated whether the energy transfer from the DE open form to the polymer conjugated backbone occurs or not. As mentioned above, the DE open form is partially degraded through the photoisomerization, which causes a decrease in intensity of the absorption band at around 250 nm even in $CHCl_3$ solution (see Figure S11, Supporting Information). Thus, if there might be any energy transfer from the DE open form to the polymer conjugated backbone, the polymer fluorescence excited by UV light of $\lambda = 250$ nm also should decrease in intensity after the photoisomerization. If not, the polymer fluorescence intensity should keep unchanged. Hence we measured excitation spectra of $CHCl_3$ solutions of the polymers in an open state, and then compared the spectra before and after 1 cycle of the photoisomerization (Figure S12, Supporting Information). The result of the excitation spectra of **P3**–**P6** showed that the PL intensity was kept unchanged even after the photoisomerization of the DE moiety (see, black arrows in Figure S12, Supporting Information). This indicates that the PL intensity is not affected by the decrease in relative amount of DE open form, i.e., there is no energy transfer from the DE open form to the polymer conjugated backbone. Because the DE open form shows no luminescence, this result implies that the energy transfer between the polymer conjugated backbone and the DE moiety may occur through the FRET mechanism, suggesting the fluorescence quenching process via FRET. However, it should be emphasized that the distance between the polymer conjugated backbone and the DE moiety is estimated to be 4–6 Å by using molecular mechanics calculation. Hence, Dexter type energy transfer, which can occur at a short distance within 10 Å via an electron-exchange process, is also regarded as an alternative mechanism of the energy transfer from the polymer backbone to the DE closed form. The detail mechanism of the fluorescence quenching still remains unclear and needs further investigation.

3. Conclusion

Full-colored fluorescent conjugated copolymers with photoswitchable emissions were synthesized by combining phenylene- and thienylene-based main chains with photochromic DE side chains. The $CHCl_3$ solutions and cast films of the polymers exhibited various colored fluorescence in visible wavelengths of 400–700 nm corresponding to their main chain structures. The fluorescence was reversibly photoswitched between emission and quenching via DE photoisomerization using external UV and visible light stimuli. The reprecipitation method with ultrasonication enabled the polymers to form spherical aggregates with diameters of 20–70 nm in water. After investigating and comparing the optical properties, the resulting nanosphere solutions were estimated to exist in an intermediate state between an isolated state in solution and an aggregated state in cast film from the viewpoint of the luminescent properties. The fluorescence photoswitching behavior was also observed in the nanosphere solutions, except for the PT derivative. The current study demonstrated that the visible fluorescence of conjugated polymers were reversibly switchable between emission and quenching using the photoisomerizing DE side chain regardless

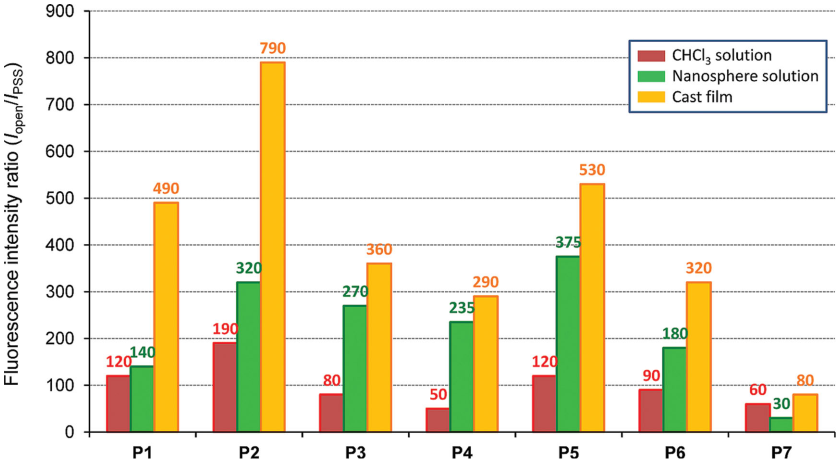

Figure 9. Fluorescence intensity ratios (I_{open}/I_{PSS}) in $CHCl_3$ solutions, nanosphere solutions, and cast films of **P1**–**P7**.

of the fluorescent color and polymer chain aggregation. It is expected that the polymers synthesized in this work will be useful for creating photoresponsive optoelectronic devices.

4. Experimental Section

Measurements: NMR spectra were measured with JEOL EX-270, JEOL AL-400, and JEOL EX-400 spectrometers. Chemical shifts were represented in parts per million downfield from tetramethylsilane (TMS) as an internal standard. High-resolution mass spectra (HRMS) were obtained by using JEOL JMS-SX102A mass spectrometer. Elemental analyses were performed by Yanako CHN Corders (MT-3, MT-5, and MT-6), JSL JM-10, Mitsubishi chemical analytech AQF-100, and Dionex ICS-1500. UV–vis absorption spectra were measured with JASCO V-570 UV/VIS/NIR spectrophotometer, and PL spectra were measured with JASCO FP-750 spectrofluorometer. All optical measurements were performed using a quartz cell or a quartz substrate. SEM was performed with JEOL JSM-7500F. The samples were coated with Pt-Pd alloy by using JEOL JFC-1600 ion coater before measurements of SEM. GPC was performed at 40 °C with a system consisting of Agilent Technologies PLgel 5 µm MIXED-D column, JASCO CO-2065 Plus column oven, JASCO UV-2070 Plus UV/VIS detector, and JASCO PU-2080 Plus HPLC pump, where the instrument was calibrated by polystyrene standard. THF was used as an eluent and the flow rate was 1.0 mL min^{-1}. Photoirradiation was carried out at room temperature by using a UV mercury lamp ($\lambda = 254$ nm, 4 W) or a visible lamp ($\lambda > 400$ nm, 100 W) as the light source. The level of DE conversion from the open form to the closed form, which is defined as {[closed form]/([open form] + [closed form])} × 100, was confirmed through ^{1}H NMR measurement in $CDCl_3$. Ratio of the open form and the closed form was determined by using the integration values of CH_2 protons neighboring a thienylene ring of DE. The relative fluorescence quantum yield (Φ) was evaluated by using quinine sulfate in 1.0 M sulfuric acid as a standard. Ultrasonication was carried out using SONICS VCX 130.

Materials: All chemicals were used as purchased. Diisopropyl azodicarboxylate (40 wt% in toluene, ≈1.9 M; DIAD), DCC, and DMAP were purchased from Tokyo Chemical Industry Co., Ltd. Triphenylphosphine (TPP) was purchased from Wako Pure Chemical Industries, Ltd. 2,5-Dibromobenzoic acid, 2-hexyl-1-decanol, 4,4′-biphenyldiboronic acid bis(neopentyl glycol) cyclic ester, 9,9-dihexylfluorene-2,7-diboronic acid bis(1,3-propanediol) cyclic ester, $Pd_2(dba)_3$, $(2\text{-furyl})_3P$ and $Pd(PPh_3)_4$ were purchased from Aldrich Co., Ltd. Methyl 4-hydroxybenzoate, sodium carbonate (Na_2CO_3), potassium hydroxide (KOH), THF, dichloromethane (CH_2Cl_2), $CHCl_3$, and methanol (MeOH) were purchased from Nacalai Tesque, Inc. THF was freshly dried and distilled over sodium benzophenone ketyl under Ar. CH_2Cl_2 was distilled over $CaCl_2$ under argon atmosphere. MERCK silica gel 60 (particle size 0.063–0.200 mm) was used to purify compounds by column chromatography. DE derivative **2** was synthesized according to previous literature.[59,60] Compounds **1**, **3**, **M1**, 2,5-dibromo-3-thenoic acid, and 5,5′-bis(trimethylstannyl)-2,2′-bithiophene were prepared according to our previous works.[49,61] 4,4′-Biphenyldiboronic acid bis(1,3-propanediol) cyclic ester was synthesized by esterification of 4,4′-biphenyldiboronic acid with 1,3-propanediol. 9,9-Dihexylfluorene-2,7-diboronic acid bis(pinacol) cyclic ester was prepared according to previous literature.[62] Photoresponsive polymers **P5** and **P6** were synthesized and reported in our previous work.[49]

Synthesis and Characterization: All syntheses were carried out under argon atmosphere. *4-(2-Hexyldecyloxy)benzoic acid (1)*: [Route **A**]: To a mixture of 2-hexyl-1-decanol (9.70 g, 40.0 mmol), TPP (11.5 g, 44.0 mmol), and methyl *p*-hydroxybenzoate (6.70 g, 44.0 mmol) in THF (70 mL) was added dropwise a solution of DIAD (23.2 mL, 44.1 mmol) in THF (20 mL) via a dropping funnel at 0 °C. The reaction mixture was stirred overnight at room temperature. After removing THF under reduced pressure, the residue was purified by column chromatography (silica gel; $CHCl_3$) to give methyl 4-(2-hexyldecyloxy)benzoate as yellow oil. The oil was dissolved in MeOH (250 mL), mixed with a solution of KOH (11.2 g, 200 mmol) in water (40 mL), and then stirred for 12 h at 50 °C. After removing MeOH under reduced pressure, HCl was added into the aqueous solution at 0 °C. The crude product was extracted with $CHCl_3$, washed with a saturated NaCl aqueous solution, and then dried over anhydrous Na_2SO_4. The precipitate was removed by filtration and the filtrate was evaporated under reduced pressure. The residue was purified by column chromatography (silica gel; $CHCl_3$) to give **1** as light yellow oil (12.8 g, 88%): ^{1}H NMR (400 MHz, $CDCl_3$, TMS): $\delta = 0.88$ (m, 6H; $(CH_2)_5C\mathit{H}_3$ and $(CH_2)_7C\mathit{H}_3$), 1.27–1.44 (m, 24H; $OCH_2CH(C\mathit{H}_2)_5CH_3$ and $OCH_2CH(C\mathit{H}_2)_7CH_3$), 1.79 (m, 1H; $OCH_2C\mathit{H}(C_6H_{13})C_8H_{17}$), 3.90 (d, *J* = 5.9 Hz, 2H; $OC\mathit{H}_2CH$), 6.93 (d, *J* = 8.8 Hz, 2H; Ph-*H* *ortho* to $OCH_2CH(C_6H_{13})C_8H_{17}$), 8.06 ppm (d, *J* = 8.8 Hz, 2H; Ph-*H* *meta* to $OCH_2CH(C_6H_{13})C_8H_{17}$); ^{13}C NMR (100 MHz, $CDCl_3$, TMS): $\delta = 14.1$, 22.7, 26.82, 26.85, 29.3, 29.6, 29.7, 30.0, 31.32, 31.34, 31.86, 31.93, 37.9, 71.2, 114.3, 121.4, 132.3, 164.0, 172.1 ppm; HRMS (ESI, *m*/*z*): [M – H^+] calcd for $C_{23}H_{38}O_3$: 361.2748; Found: 361.2754; Anal. calcd for $C_{23}H_{38}O_3$: C 76.20, H 10.57; Found: C 76.09, H 10.69. [Route **B**]: **1** was synthesized by using the same procedure with our previous study.[49]

1-{5-(2,5-Dibromo-3-thenoyloxymethyl)-2-methyl-3-thienyl}-2-(5-hydroxymethyl-2-methyl-3-thienyl)-3,3,4,4,5,5-hexafluorocyclopentene (4): To a mixture of **2** (2.50 g, 5.84 mmol), TPP (1.70 g, 6.48 mmol), and 2,5-dibromo-3-thenoic acid (1.67 g, 5.84 mmol) in THF (100 mL) was added dropwise a solution of DIAD (3.4 mL, 6.46 mmol) in THF (20 mL) via a dropping funnel at 0 °C. The reaction mixture was stirred overnight at room temperature. After removing the solvent under reduced pressure, the residue was purified by column chromatography (silica gel; $CHCl_3$) to give **4** as a pale yellow solid (1.88 g, 46%): ^{1}H NMR (400 MHz, $CDCl_3$, TMS): $\delta = 1.87$ (s, 3H; thienyl-$C\mathit{H}_3$), 1.92 (s, 3H; thienyl-$C\mathit{H}_3$), 4.75 (s, 2H; $C\mathit{H}_2OH$), 5.35 (s, 2H; $COOC\mathit{H}_2$), 6.95 (s, 1H; thienyl-*H* in DE), 7.08 (s, 1H; thienyl-*H* in DE), 7.34 ppm (s, 1H; thienyl-*H*); ^{13}C NMR (100 MHz, $CDCl_3$, TMS): $\delta = 14.46$, 14.48, 59.9, 60.9, 111.7, 119.9, 124.3, 124.6, 124.8, 128.4, 131.1, 131.6, 135.5, 142.2, 142.4, 143.6, 160.3 ppm; HRMS (ESI, *m*/*z*): [M + Na^+] calcd for $C_{22}H_{14}Br_2F_6O_3S_3$: 718.8248; Found: 718.8226; Anal. calcd for $C_{22}H_{14}Br_2F_6O_3S_3$: C 37.95, H 2.03, Br 22.95, S 13.81; Found: C 37.85, H 2.08, Br 22.88, S 13.67.

1-{5-(2,5-Dibromo-3-thenoyloxymethyl)-2-methyl-3-thienyl}-2-[5-{4-(2-hexyldecyloxy)benzoyloxymethyl}-2-methyl-3-thienyl]-3,3,4,4,5,5-hexafluorocyclopentene (M2): A solution of **1** (1.15 g, 3.17 mmol), **4** (1.66 g, 2.38 mmol), DCC (0.641 g, 3.11 mmol), and DMAP (0.324 g, 2.65 mmol) in CH_2Cl_2 (80 mL) was stirred for 60 h at room temperature. The precipitate was removed by filtration and the filtrate was evaporated under reduced pressure. The residue was purified by column chromatography (silica gel; hexane/ethyl acetate = 19:1) to give **M2** as colorless oil (2.30 g, 93%): ^{1}H NMR (400 MHz, $CDCl_3$, TMS): $\delta = 0.87$ (m, 6H; $(CH_2)_5C\mathit{H}_3$ and $(CH_2)_7C\mathit{H}_3$), 1.27–1.43 (m, 24H; $OCH_2CH(C\mathit{H}_2)_5CH_3$ and $OCH_2CH(C\mathit{H}_2)_7CH_3$), 1.79 (m, 1H; $OCH_2C\mathit{H}(C_6H_{13})C_8H_{17}$), 1.87 (s, 3H; thienyl-$C\mathit{H}_3$), 1.88 (s, 3H; thienyl-$C\mathit{H}_3$), 3.88 (d, *J* = 5.8 Hz, 2H; $OC\mathit{H}_2CH$), 5.34 (s, 2H; $COOC\mathit{H}_2$), 5.37 (s, 2H; $COOC\mathit{H}_2$), 6.90 (d, *J* = 8.8 Hz, 2H; Ph-*H* *ortho* to $OCH_2CH(C_6H_{13})C_8H_{17}$), 7.09 (s, 2H; thienyl-*H* in DE), 7.33 (s, 1H; thienyl-*H*), 7.97 (d, *J* = 8.8 Hz, 2H; Ph-*H* *meta* to $OCH_2CH(C_6H_{13})C_8H_{17}$); ^{13}C NMR (100 MHz, $CDCl_3$, TMS): $\delta = 14.1$, 14.4, 22.7, 26.80, 26.82, 29.3, 29.6, 29.7, 30.0, 31.29, 31.31, 31.8, 31.9, 37.9, 60.5, 60.9, 71.2, 111.6, 114.2, 119.9, 121.6, 124.3, 124.5, 127.6, 128.2, 131.1, 131.6, 131.7, 135.6, 136.9, 143.2, 143.7, 160.3, 163.5, 166.0 ppm; HRMS (ESI, *m*/*z*) [M + NH_4^+] calcd for $C_{45}H_{50}Br_2F_6O_5S_3$: 1058.1409; Found: 1058.1389; Anal. calcd for $C_{45}H_{50}Br_2F_6O_5S_3$: C 51.93, H 4.84, Br 15.35, S 9.24; Found: C 52.08, H 4.79, Br 15.31, S 9.21.

Photoresponsive Poly(para-phenylene) Derivative (P1): To a solution of **M1** (130 mg, 0.13 mmol), 4, 4′-biphenyldiboronic acid bis(neopentyl glycol) cyclic ester (47.2 mg, 0.13 mmol), and $Pd(PPh_3)_4$ (1.5 mg, 1.3 µmol) in THF (2 mL) was added 40% Na_2CO_3 aqueous solution (2 mL) and then the mixture was stirred overnight at 60 °C. The reaction mixture was poured into a large amount of water (300 mL) and vigorously stirred for 1 h. The resulting precipitate was collected by filtration, dissolved in minimum amount of THF (3 mL), and reprecipitated by stirring in methanol (300 mL) for 1 h. After filtration, the product was dried under vacuum to give white powder

(115 mg, 89%): ^{1}H NMR (400 MHz, $CDCl_3$, TMS): $\delta = 0.89$ (m, 6H, $(CH_2)_5CH_3$ and $(CH_2)_7CH_3$), 1.18 (m, 24H, $OCH_2CH(CH_2)_5CH_3$ and $OCH_2CH(CH_2)_7CH_3$), 1.33 (m, 1H, $OCH_2CH(C_6H_{13})C_8H_{17}$), 1.71 (s, 3H, thienyl-$CH_3$), 1.76 (s, 3H, thienyl-$CH_3$), 3.78 (d, 2H, J = 5.6 Hz, OCH_2CH), 5.15 (s, 2H, $COOCH_2$), 5.27 (s, 2H, $COOCH_2$), 6.81 (d, 2H, J = 8.2 Hz, Ph-*H* *ortho* to $OCH_2CH(C_6H_{13})C_8H_{17}$), 6.92 (s, 1H thienyl-*H* in DE), 6.98 (s, 1H, thienyl-*H* in DE), 7.16–7.77 (m, 10H, Ph-*H* in main chain), 7.88 (d, 2H, J = 8.2 Hz, Ph-*H* *meta* to $OCH_2CH(C_6H_{13})C_8H_{17}$), 8.07 (m, 1H, Ph-*H* in main chain).

Photoresponsive Poly(fluorene phenylene) Derivative (P2): The same procedure with **P1** was employed by using **M1** (172.0 mg, 0.17 mmol), 9,9-dihexylfluorene-2,7-diboronic acid bis(1,3-propanediol) cyclic ester (83.5 mg, 0.17 mmol), $Pd(PPh_3)_4$ (1.96 mg, 1.7 µmol), THF (2 mL), and 40% Na_2CO_3 aqueous solution (2 mL). The product was obtained as white powder (184 mg, 92%): ^{1}H NMR (400 MHz, $CDCl_3$, TMS): $\delta =$ 0.69 (m, 6H, $C((CH_2)_5CH_3)_2$), 0.80 (m, 6H, $(CH_2)_5CH_3$ and $(CH_2)_7CH_3$), 1.02 (m, 16H, $C(CH_2(CH_2)_4CH_3)_2$), 1.20 (m, 24H, $OCH_2CH(CH_2)_5CH_3$ and $OCH_2CH(CH_2)_7CH_3$), 1.33 (m, 1H, $OCH_2CH(C_6H_{13})C_8H_{17}$), 1.72 (s, 3H, thienyl-$CH_3$), 1.74 (s, 3H, thienyl-$CH_3$), 1.98 (m, 4H, $C(CH_2C_5H_{11})_2$), 3.79 (d, 2H, J = 6.0 Hz, OCH_2CH), 5.09 (s, 2H, $COOCH_2$), 5.28 (s, 2H, $COOCH_2$), 6.82 (d, 2H, J = 8.8 Hz, Ph-*H* *ortho* to $OCH_2CH(C_6H_{13})C_8H_{17}$), 6.88 (s, 1H thienyl-*H* in DE), 7.00 (s, 1H, thienyl-*H* in DE), 7.16–7.79 (m, 8H, Ph-*H* and fluorene-*H* in main chain), 7.89 (d, 2H, J = 8.8 Hz, Ph-*H* *meta* to $OCH_2CH(C_6H_{13})C_8H_{17}$), 8.05 (m, 1H, Ph-*H* in main chain).

Photoresponsive Poly(biphenylene thiophene) Derivative (P3): The same procedure with **P1** was employed by using **M2** (136 mg, 0.13 mmol), 4,4′-biphenyldiboronic acid bis(1,3-propanediol) cyclic ester (42.0 mg, 0.13 mmol), $Pd(PPh_3)_4$ (1.50 mg, 1.30 µmol), THF (20 mL), and 40% Na_2CO_3 aqueous solution (12 mL). The product was obtained as yellow powder (130 mg, 97%): ^{1}H NMR (400 MHz, $CDCl_3$, TMS): $\delta = 0.87$ (m, 6H, $(CH_2)_5CH_3$ and $(CH_2)_7CH_3$), 1.25 (m, 24H, $OCH_2CH(CH_2)_5CH_3$ and $OCH_2CH(CH_2)_7CH_3$), 1.36 (m, 1H, $OCH_2CH(C_6H_{13})C_8H_{17}$), 1.83 (s, 3H, thienyl-$CH_3$), 1.86 (s, 3H, thienyl-$CH_3$), 3.85 (d, 2H, J = 5.6 Hz, OCH_2CH), 5.30 (s, 2H, $COOCH_2$), 5.35 (s, 2H, $COOCH_2$), 6.87 (d, 2H, J = 8.8 Hz, Ph-*H* *ortho* to $-OCH_2CH(C_6H_{13})C_8H_{17}$), 7.07 (s, 2H thienyl-*H* in DE), 7.68 (m, 8H, Ph-*H* in main chain), 7.79 (s, 1H, thienylene-*H* in main chain), 7.96 (d, 2H, J = 8.8 Hz, Ph-*H* *meta* to $-OCH_2CH(C_6H_{13})C_8H_{17}$).

Photoresponsive Poly(fluorene thiophene) Derivative (P4): The same procedure with **P1** was employed by using **M2** (117 mg, 0.11 mmol), 9,9-dihexylfluorene-2,7-diboronic acid bis(pinacol) cyclic ester (66.0 mg, 0.11 mmol), $Pd(PPh_3)_4$ (1.27 mg, 1.1 µmol), THF (20 mL), and 40% Na_2CO_3 aqueous solution (12 mL). The product was obtained as yellow powder (122 mg, 89%): ^{1}H NMR (400 MHz, $CDCl_3$, TMS): $\delta = 0.77$ (m, 6H, $C((CH_2)_5CH_3)_2$), 0.87 (m, 6H, $(CH_2)_5CH_3$ and $(CH_2)_7CH_3$), 1.11 (m, 16H, $C(CH_2(CH_2)_4CH_3)_2$), 1.26 (m, 24H, $OCH_2CH(CH_2)_5CH_3$ and $OCH_2CH(CH_2)_7CH_3$), 1.38 (m, 1H, $OCH_2CH(C_6H_{13})C_8H_{17}$), 1.85 (s, 3H, thienyl-$CH_3$), 1.87 (s, 3H, thienyl-$CH_3$), 2.06 (m, 4H, $C(CH_2C_5H_{11})_2$), 3.86 (d, 2H, J = 5.2 Hz, OCH_2CH), 5.29 (s, 2H, $COOCH_2$), 5.36 (s, 2H, $COOCH_2$), 6.89 (d, 2H, J = 8.4 Hz, Ph-*H* *ortho* to $OCH_2CH(C_6H_{13})C_8H_{17}$), 7.07 (s, 1H thienyl-*H* in DE), 7.10 (s, thienyl-*H* in DE), 7.45–7.79 (m, 7H, fluorene-*H* and thienylene-*H* in main chain), 7.96 (d, 2H, J = 8.4 Hz, Ph-*H* *meta* to $OCH_2CH(C_6H_{13})C_8H_{17}$).

Photoresponsive Polythiophene Derivative (P7): A solution of **M2** (104 mg, 0.10 mmol), $Pd_2(dba)_3$ (0.92 mg, 1.00 µmol), and $(2\text{-furyl})_3P$ (0.93 mg, 4.00 µmol) in THF (2 mL) was stirred at 50 °C for 30 min, followed by addition of 5,5′-bis(trimethylstannyl)-2,2′-bithiophene (49.2 mg, 0.10 mmol). After stirred at 50 °C for 25 h, the reaction mixture was poured into a large amount of methanol (100 mL) containing HCl and then vigorously stirred for 3 h. The resulting precipitate was collected by filtration, dissolved in minimum amount of THF (3 mL), and reprecipitated by stirring in methanol (100 mL) for 30 min. After filtration, the product was dried under vacuum to give dark red powder (90 mg, 86%): ^{1}H NMR (400 MHz, $CDCl_3$, TMS): $\delta = 0.85$ (t, J = 6.6 Hz, 6H; $(CH_2)_5CH_3$ and $(CH_2)_7CH_3$), 1.24–1.42 (m, 24H; $OCH_2CH(CH_2)_5CH_3$ and $OCH_2CH(CH_2)_7CH_3$), 1.74 (m, 1H; $OCH_2CH(C_6H_{13})C_8H_{17}$), 1.89 (br, 6H; thienyl-CH_3), 3.82 (d, J = 5.2 Hz, 2H; OCH_2CH), 5.34 (br, 4H; $COOCH_2$), 6.78 (br, 2H; thienylene-*H* in main chain), 6.86 (d, J = 8.8 Hz, 2H; Ph-*H* *ortho* to $OCH_2CH(C_6H_{13})C_8H_{17}$), 7.11 (br, 2H; thienyl-*H* in DE), 7.21 (br, 3H; thienylene-*H* in main chain), 7.95 (d, J = 8.8 Hz, 2H; Ph-*H* *meta* to $OCH_2CH(C_6H_{13})C_8H_{17}$).

Supporting Information

Supporting Information is available from the Wiley Online Library or from the author.

Acknowledgments

The authors thanked Kazuya Tamura for his valuable cooperation in synthesis and spectroscopic measurements. This work was supported by Grants-in-Aid for Science Research (A) (Grant No. 25246002) from the Ministry of Education, Culture, Sports, Science and Technology, Japan.

Received: January 12, 2015
Revised: February 27, 2015

[1] J. H. Burroughes, D. D. C. Bradley, A. R. Brown, R. N. Marks, K. Mackay, R. H. Friend, P. L. Burns, A. B. Holmes, *Nature* **1990**, *347*, 539.
[2] R. H. Friend, R. W. Gymer, A. B. Holmes, J. H. Burroughes, R. N. Marks, C. Taliani, D. D. C. Bradley, D. A. Dos Santos, J. L. Bredas, M. Logdlund, W. R. Salaneck, *Nature* **1999**, *397*, 121.
[3] C. V. Hoven, A. Garcia, G. C. Bazan, T. Q. Nguyen, *Adv. Mater.* **2008**, *20*, 3793.
[4] S. Guenes, H. Neugebauer, N. S. Sariciftci, *Chem. Rev.* **2007**, *107*, 1324.
[5] D. T. McQuade, A. E. Pullen, T. M. Swager, *Chem. Rev.* **2000**, *100*, 2537.
[6] S. W. Thomas III, G. D. Joly, T. M. Swager, *Chem. Rev.* **2007**, *107*, 1339.
[7] H. E. A. Huitema, G. H. Gelinck, J. B. P. H. van der Putten, K. E. Kuijk, C. M. Hart, E. Cantatore, P. T. Herwig, A. J. J. M. van Breemen, D. M. de Leeuw, *Nature* **2001**, *414*, 599.
[8] C. D. Dimitrakopoulos, P. R. L. Malenfant, *Adv. Mater.* **2002**, *14*, 99.
[9] A. C. Grimsdale, K. L. Chan, R. E. Martin, P. G. Jokisz, A. B. Holmes, *Chem. Rev.* **2009**, *109*, 897.
[10] K. Akagi, *Bull. Chem. Soc. Jpn.* **2007**, *80*, 649.
[11] L. A. P. Kane-Maguire, G. G. Wallace, *Chem. Soc. Rev.* **2010**, *39*, 2545.
[12] K. Watanabe, K. Suda, K. Akagi, *J. Mater. Chem. C* **2013**, *1*, 2797.
[13] K. Watanabe, K. Akagi, *Sci. Technol. Adv. Mater.* **2014**, *15*, 044203.
[14] A. Qin, J. W. Y. Lam, B. Z. Tang, *Prog. Polym. Sci.* **2012**, *37*, 182.
[15] R. Hu, J. Luis Maldonado, M. Rodriguez, C. Deng, C. K. W. Jim, J. W. Y. Lam, M. M. F. Yuen, G. Ramos-Ortiz, B. Z. Tang, *J. Mater. Chem.* **2012**, *22*, 232.
[16] X. Liu, J. Jiao, X. Jiang, J. Li, Y. Cheng, C. Zhu, *J. Mater. Chem. C* **2013**, *1*, 4713.
[17] M. Irie, *Chem. Rev.* **2000**, *100*, 1685.
[18] K. Matsuda, M. Irie, *J. Photochem. Photobiol. C* **2004**, *5*, 169.
[19] H. Tian, S. J. Yang, *Chem. Soc. Rev.* **2004**, *33*, 85.
[20] H. Tian, S. Wang, *Chem. Commun.* **2007**, 781.
[21] Z. Zhang, X. Liu, Z. Li, Z. Chen, F. Zhao, F. Zhang, C. Tung, *Adv. Funct. Mater.* **2008**, *18*, 302.
[22] P. Zacharias, M. C. Gather, A. Koehnen, N. Rehmann, K. Meerholz, *Angew. Chem. Int. Ed.* **2009**, *48*, 4038.
[23] H. K. Bisoyi, Q. Li, *Acc. Chem. Res.* **2014**, *47*, 3184.

[24] Y. Li, M. Wang, A. Urbas, Q. Li, *J. Mater. Chem. C* **2013**, *1*, 3917.
[25] Y. Li, C. Xue, M. Wang, A. Urbas, Q. Li, *Angew. Chem. Int. Ed.* **2013**, *52*, 13703.
[26] K. Rameshbabu, A. Urbas, Q. Li, *J. Phys. Chem. B* **2011**, *115*, 3409.
[27] K. Rameshbabu, L. Zou, C. Kim, A. Urbas, Q. Li, *J. Mater. Chem.* **2011**, *21*, 15673.
[28] T. Fukaminato, M. Irie, *Adv. Mater.* **2006**, *18*, 3225.
[29] T. B. Norsten, N. R. Branda, *Adv. Mater.* **2001**, *13*, 347.
[30] T. B. Norsten, N. R. Branda, *J. Am. Chem. Soc.* **2001**, *123*, 1784.
[31] S. Lim, B. An, S. D. Jung, M. Chung, S. Y. Park, *Angew. Chem. Int. Ed.* **2004**, *43*, 6346.
[32] T. Kawai, T. Sasaki, M. Irie, *Chem. Commun.* **2001**, 711.
[33] G. Y. Jiang, S. Wang, W. F. Yuan, L. Jiang, Y. L. Song, H. Tian, D. B. Zhu, *Chem. Mater.* **2006**, *18*, 235.
[34] L. Giordano, T. M. Jovin, M. Irie, E. A. Jares-Erijman, *J. Am. Chem. Soc.* **2002**, *124*, 7481.
[35] S. Murase, M. Teramoto, H. Furukawa, Y. Miyashita, K. Horie, *Macromolecules* **2003**, *36*, 964.
[36] M. Berberich, A. Krause, M. Orlandi, F. Scandola, F. Würthner, *Angew. Chem. Int. Ed.* **2008**, *47*, 6616.
[37] S. Yagai, K. Iwai, T. Karatsu, A. Kitamura, *Angew. Chem. Int. Ed.* **2012**, *51*, 9679.
[38] T. Kawai, T. Kunitake, M. Irie, *Chem. Lett.* **1999**, *28*, 905.
[39] C. P. Harvey, J. D. Tovar, *Polym. Chem.* **2011**, *2*, 2699.
[40] Q. Luo, H. Cheng, H. Tian, *Polym. Chem.* **2011**, *2*, 2435.
[41] T. Kawai, Y. Nakashima, M. Irie, *Adv. Mater.* **2005**, *17*, 309.
[42] A. Kaeser, A. P. H. J. Schenning, *Adv. Mater.* **2010**, *22*, 2985.
[43] Z. Tian, J. Yu, C. Wu, C. Szymanski, J. McNeill, *Nanoscale* **2010**, *2*, 1999.
[44] E. J. Harbron, C. M. Davis, J. K. Campbell, R. M. Allred, M. T. Kovary, N. J. Economou, *J. Phys. Chem. C* **2009**, *113*, 13707.
[45] C. M. Davis, E. S. Childress, E. J. Harbron, *J. Phys. Chem. C* **2011**, *115*, 19065.
[46] J. Finden, T. K. Kunz, N. R. Branda, M. O. Wolf, *Adv. Mater.* **2008**, *20*, 1998.
[47] N. Anwar, T. Willms, B. Grimme, A. J. C. Kuehne, *ACS Macro Lett.* **2013**, *2*, 766.
[48] Y. Chan, M. E. Gallina, X. Zhang, I. Wu, Y. Jin, W. Sun, D. T. Chiu, *Anal. Chem.* **2012**, *84*, 9431.
[49] H. Hayasaka, K. Tamura, K. Akagi, *Macromolecules* **2008**, *41*, 2341.
[50] H. Hayasaka, T. Miyashita, K. Tamura, K. Akagi, *Adv. Funct. Mater.* **2010**, *20*, 1243.
[51] J. Bu, K. Watanabe, H. Hayasaka, K. Akagi, *Nat. Commun.* **2014**, *5*, 3799.
[52] B. M. W. Langeveld-Voss, R. A. J. Janssen, M. P. T. Christiaans, S. C. J. Meskers, H. P. J. M. Dekkers, E. W. Meijer, *J. Am. Chem. Soc.* **1996**, *118*, 4908.
[53] E. Peeters, A. Delmotte, R. A. J. Janssen, E. W. Meijer, *Adv. Mater.* **1997**, *9*, 493.
[54] B. M. W. Langeveld-Voss, R. A. J. Janssen, E. W. Meijer, *J. Mol. Struct.* **2000**, *521*, 285.
[55] N. Kurokawa, H. Yoshikawa, N. Hirota, K. Hyodo, H. Masuhara, *ChemPhysChem* **2004**, *5*, 1609.
[56] S. Mukamel, S. Tretiak, T. Wagersreiter, V. Chernyak, *Science* **1997**, *277*, 781.
[57] A. Kohler, D. A. dos Santos, D. Beljonne, Z. Shuai, J. L. Bredas, A. B. Holmes, A. Kraus, K. Mullen, R. H. Friend, *Nature* **1998**, *392*, 903.
[58] J. Yu, D. H. Hu, P. F. Barbara, *Science* **2000**, *289*, 1327.
[59] S. L. Gilat, S. H. Kawai, J. M. Lehn, *Chem. Eur. J.* **1995**, *1*, 275.
[60] G. Sevez, J. Gan, J. Pan, X. Sallenave, A. Colin, H. Saadoui, A. Saleh, F. Voegtle, J.-L. Pozzo, *J. Phys. Org. Chem.* **2007**, *20*, 888.
[61] K. Watanabe, I. Osaka, S. Yorozuya, K. Akagi, *Chem. Mater.* **2012**, *24*, 1011.
[62] S. P. Dudek, M. Pouderoijen, R. Abbel, A. P. H. J. Schenning, E. W. Meijer, *J. Am. Chem. Soc.* **2005**, *127*, 11763.